IMPROVING THE SiO_2 EQUATION OF STATE WITH SHOCK AND POST-SHOCK TEMPERATURES

Kaitlyn M. Amodeo[1], Erik J. Davies[2], Sarah T. Stewart[1], and Dylan K. Spaulding[1], [1]University of California, Davis (kamodeo@ucdavis.edu), [2]Lawrence Livermore National Laboratory

Introduction: Planet formation and evolution involves high energy impacts capable of melting and vaporizing silicate mantles [1, 2]. SiO_2 is an important end-member phase and reference material. At present, researchers lack a wide-ranging equation of state model for SiO_2 that accurately captures the temperatures on the shock Hugoniot and post-shock states. The quartz and fused silica (amorphous SiO_2) equations of state (EOS) can be improved with additional lab data, particularly *in situ* shock and post-shock temperatures in the region where these materials undergo shock melting.

Along with their utility as compositional end-member minerals, these materials are often used in a variety of shock experiments as windows and standards for impedance matching and thermal emission [3, 4]. Thus, improving the laboratory measurements and modeled data for these materials provides better standard references. Previous studies using gas guns [5, 6] and laser-driven shocks [3] sampled this region, but little data is available in the superheating region of the Hugoniot and liquid region along the vapor curve. Additional data in this region provides insight to both the transition of SiO_2 into the liquid phase in a shocked state as well as the onset of melting and vaporization upon release.

The analytic equations of state code package (ANEOS) is frequently used by the planetary science community as it is capable of spanning the substantial temperature and pressure range achieved in natural impact phenomenon [7]. The code package has multiple features that enable modeling of solids, liquids, gases and plasmas. For most natural materials, the code package cannot accurately model the entire pressure-temperature range needed. As a result, each developer must make decisions about which features to use in the code package and which regions to fit more accurately.

These decisions lead to a set of material parameters for use with a specific version of the ANEOS code that are constrained by data in some regions of phase space. Melosh [7] made updates to ANEOS using SiO_2 where a Mie-type potential is used for the solid phase and molecular clusters are used for the vapor phase (M-ANEOS). At present, the available ANEOS models for silica have significant discrepancies in the melt region and liquid-vapor phase boundary compared to laboratory observations. Figure 1 shows currently available ANEOS model Hugoniot and vapor domes for SiO_2 alongside lab data [6, 11, 8].

This study focuses on taking shock and post-shock temperatures of quartz and fused silica in the pressure range where these materials undergo superheating and melting, approximately 55-130 GPa using multiple pyrometry systems. Here, we describe our shock pyrometry experiments on fused silica as well as plans for improving the model equation of state.

Laboratory Methods: Shock data were collected at the UC Davis Shock Compression Laboratory using the 80/25 mm two-stage light gas gun. This facility is capable of producing high-precision planar shock waves though geologic materials at impact velocities up to ~ 7 km s^{-1} or ~ 130 GPa in silica. Specialized optical pyrometry and velocimetry diagnostics allows us to measure impact velocity, shock velocity, and shock/post-shock temperatures [12].

A typical sample is a 25 mm diameter disk with a thickness of 3 mm. The fused quartz had a density of

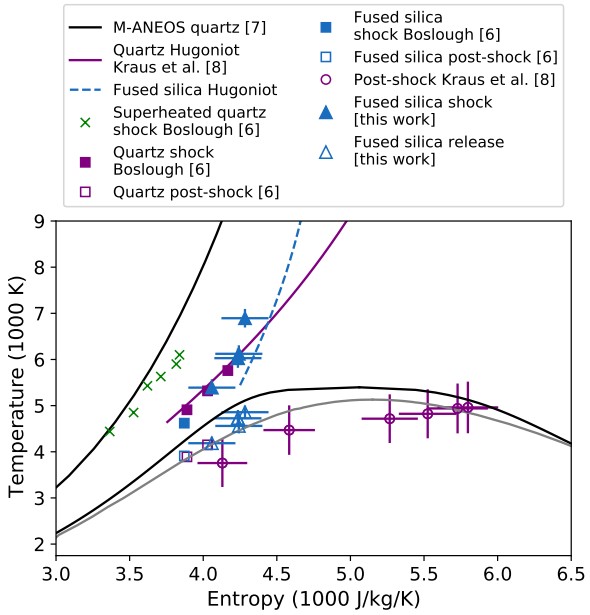

Figure 1: Plot of shock Hugoniots and the vapor dome for silica: M-ANEOS Hugoniot from Melosh [7] (black lines), quartz Hugoniot and vapor dome from Kraus et al. [8] (purple and gray lines), and fused silica Hugoniot using entropy from Kraus et al. [8] and temperatures from Brygoo et al. [9] (dashed blue line). Notably, the model Hugoniots do not include the melt curve or the superheating phenomenon. Silica entropies from Luo et al. [10] in the superheated region (green X's) and from Kraus et al. [8] in the liquid region.

2.181 ± 0.002 g/cc. The samples are mounted in a secondary vacuum chamber to avoid contamination of spectral radiance data from residual shocked gas in the gun's target tank.

Temperature was measured using three distinct fiber-coupled pyrometry systems. The first system consists of four near-infrared (NIR) InSb detectors centered at 1.8, 2.3, 3.5, and 4.8 μm. Next, are two visible light detectors (Si photodiodes), with a 600 nm long pass filter and a 700 nm short pass filter. The third is a Streaked Visible Spectroscopy (SVS) system covering a broad, continuous spectrum of visible wavelengths from 350 to 850 nm [13]. The time-dependent thermal emission data are analyzed as described in Luo et al. [11] which corrects the spectral radiance for wavelength-dependent absorption. The combination of these systems allows us to determine calibrated shock and post-shock radiance over a broad wavelength range that are converted to temperature with the Planck function.

ANEOS improvements: The improvements to ANEOS follow those described in Stewart et al. [14] in which the forsterite EOS was improved using additional lab data. These improvements include the addition of a user adjustable heat capacity; the original heat capacity in ANEOS is $3N_0kT$, or the classical Dulong-Petit limit. This limit is appropriate for the solid phase, but is not appropriate for the melt or supercritical fluid. As shown in Fig. 1, the M-ANEOS Hugoniot [7] is in fairly good agreement with quartz shock temperature measurements [6] in the superheated regime. However, there is strong disagreement with this Hugoniot and the shock temperature data inferred to be in the liquid field (those points at higher specific entropies).

With the updated ANEOS code package, the heat capacity can now be adjusted with an empirical term f_{cv} such that the limiting heat capacity is $3f_{cv}N_0kT$. Currently, changing this term leads to a poorer quality fit in the solid region. Future work will use the ANEOS package to make multi-phase EOS tables that use the appropriate thermal models for the solid and fluid phases.

Preliminary results and future work: A preliminary dataset on fused silica is shown in Fig. 1. Our shock temperature data on fused silica are slightly offset from the Hugoniot predicted by [8]. The combined post-shock temperature data will be used to improve the model liquid-vapor boundary. The combination of shock temperatures with static thermodynamic data will be used to improve the calculation of entropy on the Hugoniot.

Note that our measured radiance in silica over the entire visible to near-infrared range cannot be fit by an ideal greybody. We infer the presence of wavelength-dependent material properties that introduce additional uncertainties into the inference of the sample temperature. These uncertainties are reflected in our error bars.

In the data shown in Fig. 1, the post-shock temperatures assume an emissivity of 1; however we infer wavelength dependence on this parameter. We note that in previous work, the inferred shock front emissivity varied noticably between experiments [5]. Inclusion of infrared wavelengths in thermal radiance measurements indicates that the uncertainties in the inferred temperature are larger than typically reported for shock temperature measurements using visible data alone.

Conclusion: Shock and post-shock temperature data for quartz and fused silica can provide extremely useful thermodynamic data that are needed to improve equation of state models over the wide range of pressures and temperatures attained in planetary impacts. Adjustments to the user defined heat capacity in an updated version of ANEOS will create a better multi-phase EOS for silica.

Acknowledgements: This work was supported NASA grant NNX15AH54G, NASA grant NNX16AP35H (EJD), Simons Foundation grant 55420, and UC Office of the President grant LFR-17-449059, prepared by LLNL under Contract DE-AC52-07NA27344.

References: **[1]** J. Chambers. In: *Exoplanets*. 2010. **[2]** R. M. Canup. (2008), ***PTRS 366***. **[3]** D. G. Hicks et al. (2005), *Physics of Plasmas* ***12***. **[4]** M. D. Knudson and M. P. Desjarlais. (2009), ***PRL 103***. **[5]** G. A. Lyzenga and T. J. Ahrens. (1980), ***GRL 7***. **[6]** M. B. Boslough. (1988), ***JGR 93***. **[7]** H. J. Melosh. (2007), *Meteoritics & Planetary Science* ***42***. **[8]** R. G. Kraus et al. (2012), *JGR: Planets* ***117***. **[9]** S. Brygoo et al. (2007), *Nature Materials* ***6***. **[10]** S. N. Luo et al. (2003), *Journal of Geophysical Research: Solid Earth* ***108***. **[11]** S. N. Luo et al. (2004), *JGR: Solid Earth* ***109***. **[12]** S. T. Stewart and D. K. Spaulding. In: *LPSC XLVIII*. (2017). **[13]** E. J. Davies, D. K. Spaulding, and S. T. Stewart. In: *SCCM19*. (2019). **[14]** S. T. Stewart et al. In: *SCCM19*. (2019).